Resolved Particle Simulations of Microsphere/Cell-based Bioanalytic Systems

K. Pant, B.F. Romanowicz and S. Sundaram*

CFD Research Corporation
215 Wynn Drive, Huntsville, AL 35805
*Corresponding author, e-mail: sxs@cfdrc.com

ABSTRACT

Microsphere and cell-based assays are emerging as the platform of choice for rapid quantitation of biomolecular interactions in bioagent detection, clinical diagnosis, drug therapy, etc. [1,2] Traditional assay designs have been driven by expensive trial-and-error experimentation. The availability of high-fidelity simulation tools for these complex microsystems can help accelerate the design cycle significantly. However, current models rely on a point particle approximation and are incapable of describing large particle dynamics or biochemical coupling adequately. In a novel development, we have successfully developed computational models for finite-sized cells/bead assay design within a multiphysics biomicrofluidic simulation software suite, CFD-ACE+. The developed models fully integrate large bead dynamics, convective-diffusive analyte transport and biomolecular binding on bead surface. In this paper, we present the modeling framework, along with several validation and demonstration case studies.

Keywords: microsphere, cell, assay, design, resolved particle simulations

1 INTRODUCTION

The use of whole cells in microfluidic platforms to study biological interactions has been growing rapidly. Microspheres (or beads) are also used extensively in a variety of such applications as support structures for antibodies, proteins, DNA, etc. Microsphere- and cell-based assays provide several key benefits over conventional surface-derivatized assays including: (1) improved mixing and contacting, (2) ease of processing, e.g., cytometry, elution, etc., (3) ready multiplexing (4) continuous monitoring, and (5) enhanced functionality with magnetic/electric fields.

Traditionally, microsphere- and cell-based assay design development practices have been based on expensive, time-consuming, trial-and-error experimentation. The emergence of high fidelity, multiphysics simulations based analysis represents a shifting paradigm in bead/cell assay design [3]. A computational prototyping approach can be employed to screen design concepts, optimize performance and shorten the design cycle with tremendous savings in time and cost. However, widespread use of simulation-enabled design has been limited by two key technological deficiencies: (1) inaccurate and inadequate representation of momentum and analyte exchange between beads and suspending fluid. This shortcoming is especially felt for large beads (relative to flow length scales) since conventional Lagrangian models rely upon a point particle approximation, where the volume of the buffer displaced by cell/bead is neglected. This clearly is not a valid assumption for microfluidic systems where bead/cell size is comparable to flow/system length scales, and (2) lack of bio-kinetic adsorption mechanisms and appropriate rate constants applicable to different classes of bio-molecular interactions.

In this paper, we present a recent development for high-fidelity design analysis of microsphere- and cell-based bioanalytic microsystems. The modeling framework couples an enhanced Lagrangian particle tracking methodology for finite-size particles with buffer/analyte transport and a suite of biochemistry models for surface binding. Flow features at bead/cell length scales are resolved using a novel surface marker point approach (termed *Resolved Particle Simulations* or *RPS)* to track the surface of the particle. Non-uniformities in surface coverage, shear stress, etc. on particle surface are computed implicitly in a finite volume formulation. The modeling approach is validated and demonstrated for different problems.

2 MODEL FORMULATION

Characterization of interactions between bulk (buffer/analyte) and bead/cell-surface immobilized biomolecules requires a fundamental understanding of (a) coupled fluid and bead motion (fluid-solid momentum transfer), and (b) analyte transport and binding (fluid-solid mass transfer). Mathematical models employed in RPS follow a generalized multiphase formalism [4] and are discussed next.

2.1 Buffer Transport

Buffer transport in the bulk is governed by the conservation of mass and momentum and is mathematically described by continuity and Naviér-Stokes equations as [5]:

$$\frac{\partial \alpha_c u_i}{\partial x_i} = 0 \qquad (1)$$

$$\frac{\partial \alpha_c \rho_c u_i}{\partial t} + \frac{\partial \alpha_c \rho_c u_j u_i}{\partial x_j} = -\alpha_c \frac{\partial P}{\partial x_i} + \frac{\partial \alpha_c \tau_{ij}}{\partial x_j} - \beta_V (u_i - v_i) + \alpha_c \rho_c g_i \quad (2)$$

where u, ρ_c, P and g are the buffer velocity, density, pressure and gravity respectively and v is bead/cell velocity. Note that the volume displaced by the particles is accounted for by including the buffer volume fraction or porosity, α_c. Fluid stresses (τ_{ij}) and interphase momentum transfer coefficient (β_V) are expressed in terms of basic variables using constitutive relations.

2.2 Analyte Transport

Analyte transport in the bulk (buffer) solution occurs due to convective (governed by convective flow rate) and diffusive mechanisms (determined by mass diffusivity of analyte). The mass conservation of analyte is written as [5]:

$$\frac{\partial \alpha_c C}{\partial t} + \frac{\partial \alpha_c u_j C}{\partial x_j} = D \frac{\partial^2 \alpha_c C}{\partial x_i \partial x_j} + S \quad (3)$$

where C, D and S are the analyte concentration, diffusivity and source/sink term (due to surface binding), respectively. The analyte transport equation is also modified to account for volume exclusion due to finite-sized particles.

2.3 Bead/Cell Motion

The equation of motion of a particle in a Lagrangian framework is represented as [6]:

$$\frac{\partial v_i}{\partial t} = A_D + g_i + \sum_{i \neq j} A_{c,ij} \quad (4)$$

where A_D is the bead acceleration due to fluidic drag, g_i is the body force and $A_{c,ij}$ is the collisional acceleration. In traditional trajectory methods, the drag force on a particle is obtained from a uniform flow over a sphere approach, which is invalid for large particles due to strong spatial variations in the flow field.

In RPS, the bead/cell is represented by a center of mass location and a pre-specified number of surface marker points as shown in figure 1. The region occupied by the bead is blocked off to the fluid using the porosity variable and tangential no-slip and zero normal flux boundary conditions are imposed on the surface of the particle. Drag force on the bead is computed by explicit numerical integration along the surface as:

$$F_D = \sum_{k=1}^{N} \left(-p_k + \boldsymbol{\tau}_{ij,k} \cdot \vec{\mathbf{n}}_k \right) \Delta S_k \quad (5)$$

where p_k is pressure at marker point cell k, $\boldsymbol{\tau}_{ij,k}$ is stress tensor at marker point cell k, n_k is the outward normal at marker point k, ΔS_k is the surface area associated with marker point k, and N is the total number of marker points. The RPS approach is also different from the technique reported in [7], as it does not involve expensive remeshing.

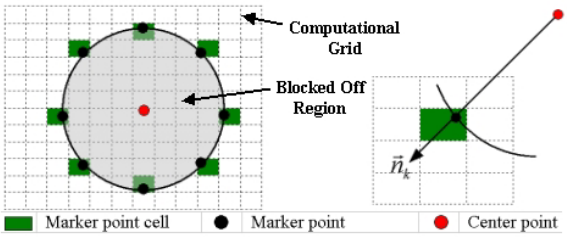

Figure 1. Drag calculation in Resolved Particle Simulations

2.4 Surface Binding

Analyte-receptor interaction takes place at the bead/cell surface and is modeled using a suite of biochemistry models including (a) enzyme kinetics, including Michaelis-Menten, substrate inhibition/activation, competitive/non-competitive inhibition and multiple substrate kinetics, (b) protein adsorption/DNA hybridization with arbitrary order kinetics, and (c) user-specified kinetics. Temporal evolution of bead/cell surface coverage is tracked. For pseudo first-order kinetics (Langmuir adsorption model), the evolution equation can be written as

$$\frac{d\theta}{dt} = K_{on} C_s (1 - \theta) - K_{off} \theta \quad (6)$$

where θ is the surface coverage fraction and K_{on} and K_{off} are the adsorption and desorption rate constants, respectively. A mass balance between the arrival flux at bead/cell surface (due to transport) and production/consumption rate (due to reaction) is imposed for each analyte in the system.

2.5 Particle Interactions

Particle-particle interactions are resolved using either (a) hard sphere collisions [5,8] or (b) inverse polynomial soft potential approach. The latter is based on Molecular Dynamics (MD) methodology and accounts for particle collisions using a short range repulsive force. The force on bead i due to bead j is given by

$$\vec{F}_{ij} = \begin{cases} \vec{0}, & if \ \left|\vec{r}_{ij}\right| > d + \rho \\ \varepsilon \left(\frac{d}{\left|\vec{r}_{ij}\right|} \right)^n \frac{\vec{r}_{ij}}{\left|\vec{r}_{ij}\right|}, & if \ \left|\vec{r}_{ij}\right| \leq d + \rho \end{cases} \quad (7)$$

where $\vec{r}_{ij}$ is the separation vector between i and j, ε is the force scaling (stiffness) parameter and ρ is the force range. The total net force acting on ith bead is obtained by summing up the contributions from all the other beads within the computational domain. The characteristics of the force are tailored such that it acts only over a short range to prevent bead overlap by acting continuously over time, which enhances model stability and robustness.

3 MODEL VALIDATION

The Resolved Particle Simulations modeling framework was validated using two different canonical flows: (1) Settling under gravity, and (2) Flow over a cylinder. The results from these studies are discussed next.

3.1 Settling Under Gravity

The first validation case was taken be that of a particle (diameter D) settling in a stagnant fluid under the influence of gravitational field as shown in figure 2. The two-dimensional planar computational domain was taken to be $15D$ in height and $10D$ in width, where D is the particle diameter. The sides of the computational domain were specified to be symmetry boundaries and the top and bottom were taken to be entrainment boundaries. The initial velocity of the particle was taken to be zero.

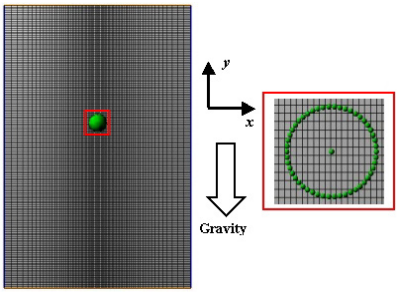

Figure 2. Particle settling under gravity

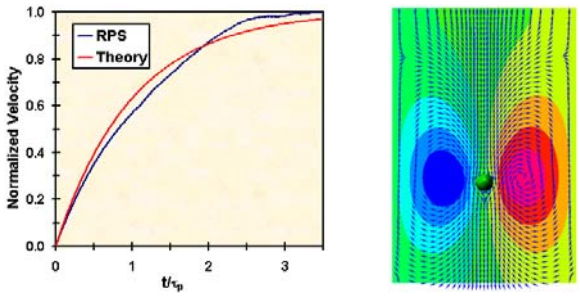

Figure 3. (a) Particle normalized velocity (b) Flow pattern

Particle velocity, normalized with respect to the predicted settling velocity, is presented in figure 3(a), along with an exponential rise curve, based on the aerodynamic response time (τ_p) of the particle. The computed velocity increases initially due to an imbalance in the forces acting on the particle. Particle location, streamfunction and velocity vectors at t=1.91 τ_p is shown in figure 3(b). Note that as the particle pushes the fluid down, it sets up a recirculatory flow pattern within the computational domain.

3.2 Flow over a Cylinder

A second validation case for was taken to be flow over a cylinder. Both explicitly meshed (direct) and RPS calculations were carried out for a cylinder of diameter (D) exposed to a freestream velocity (U_0). The Reynolds number based on freestream velocity and cylinder diameter was taken to be 100. Flow velocities and pressure were monitored at three probes locations (shown in figure 4) downwind of the cylinder.

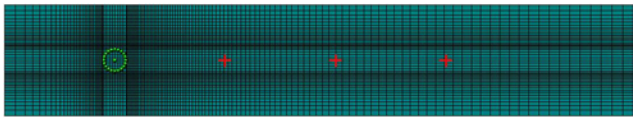

Figure 4. Flow over a cylinder (probe locations in red)

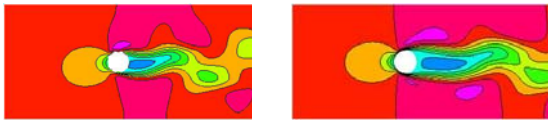

Figure 5. (a) RPS (b) Direct simulation

Planar visualizations of streamwise velocity contours are presented in figure 5. The results from RPS are in good qualitative agreement with direct calculations. To quantitatively compare the results, the shedding frequency for the two cases was computed and averaged over the three probe locations. The shedding frequency from RPS (0.182 s^{-1}) was found to be within 3% of the shedding frequency for direct calculations (0.177 s^{-1}).

4 SOFTWARE DEMONSTRATION

Resolved Particle Simulations provide for unprecedented fidelity for analysis of microsphere- and cell-based assays. As a demonstration case, we study here the evolution of surface coverage non-uniformities in a trapped bead binding platform. An axisymmetric planar representation (shown in figure 6) of a typical fluidization platform was selected for these demonstration calculations. The device consists of antibody-coated microspheres suspended in a chamber and trapped between two mechanical screens. Sample is injected through an inlet at the bottom of the device and is contacted with the beads in the chamber. The chamber was taken to be 16.6 mm in diameter and 80 mm long. Twenty (20) 3 mm diameter beads were seeded randomly throughout the domain between the two screens. Note that the beads are several times (6-8 times) bigger than the computational cell size. The assay of *E. coli* binding to its probe was studied for these calculations.

Time snapshots of bead locations and fluid streamlines are presented in figure 6. The prescribed fluid velocity is not large enough to adequately fluidize the bead bed and the particles exhibit hindered settling in the chamber. The primary advantage of RPS over traditional approaches lies in accurate and explicit resolution of flow around the particle. This is clearly demonstrated by the wake formation behind the beads and the deflection of fluid streamlines around the beads. This effect cannot be captured in such detail with traditional point particle methods.

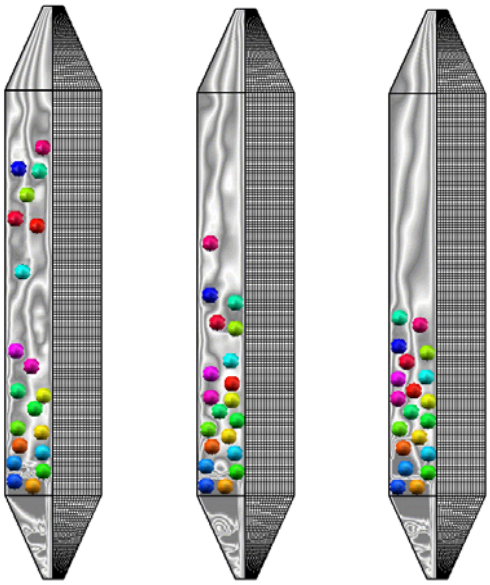

Figure 6. RPS of trapped bead assay
(a) t=0.5s, (b) t=1.0s, t=2.0s

Non-uniform binding on the bead surface is also captured effectively using RPS (see figure 7). The surface marker points are colored by surface coverage (θ) – for this scale, θ is defined as fractional coverage based on the surface area associated with the marker point. Analyte contours are plotted in the background with red indicating high analyte concentration and blue indicating low analyte concentration. The side of the microspheres exposed to higher sample concentrations displays higher surface coverage. Obviously, this has implications for signal to noise ratios during flow cytometry. Note that particle rotation, which would mitigate this phenomenon, is not included in these calculations. Such high-resolution analysis of microsphere/cell-based bioanalytic systems can be employed to evaluate design concepts and quantitatively explore design parameter space in a cost-effective manner.

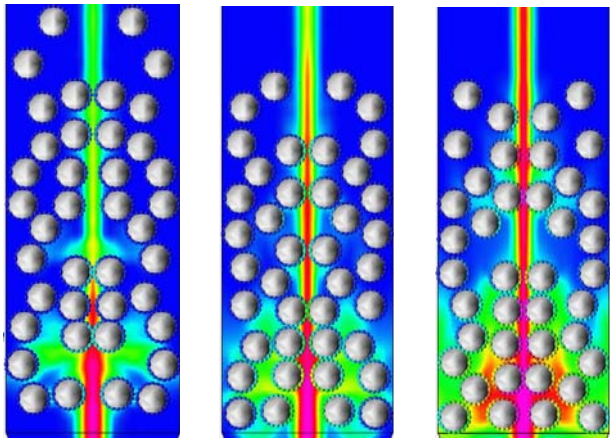

Figure 7. Non-uniform surface binding
(a) t=0.5s, (b) t=1.0s, t=2.0s

5 CONCLUSIONS

Resolved Particle Simulations (RPS), a novel methodology for high-fidelity design of microsphere- and cell-based assays was developed and implemented within CFD-ACE+, a widely used general-purpose biomicrofluidic design software from CFDRC. The computational framework combines large particle dynamics with a suite of biochemistry models and buffer/analyte transport to provide for unprecedented details of flow features and surface coverage. The developed models were validated for different canonical flows and numerical predictions were found to be in good agreement with analytical results and direct computations. Demonstration calculations with a trapped bead binding platform were performed using RPS. The computational model was able to predict hindered settling of particles and non-uniform surface binding satisfactorily. In summary, CFDRC has successfully developed high-fidelity computational models for simulating biochemical reactions on flowing, large beads. Such an analysis tool can be used with great impact to develop a fundamental understanding of the biochemical and/or transport processes involved, optimize assay design, and screen new concepts for improvement.

ACKNOWLEDGEMENT

The authors gratefully acknowledge support for this work under NSF SBIR program (DMI-0216507, Program Monitor: Dr. Om Sahai).

REFERENCES

[1] Sundaram, S. & Makhijani, V.B., SIMBAD Phase I Final Report, Lockheed Martin/DARPA, 2000.
[2] Weimer, B. C., Walsh, M. K., Beer, C., Koka, R. & Wang, X., *Appl. Env. Microbiol.*, 67, 1300, 2001.
[3] Pandian, P.B., Shah, K.B., Sundaram, S. & Makhijani, V.B., *MSM International Conference*, 92, 2002.
[4] Duchanoy, C. & Jongen, T., *Comput. Fluids*, 32, 1453, 2003.
[5] Crowe, C.T., Sommerfeld, M., & Tsuji, Y., *Multiphase Flows with Droplets and Particles*, CRC Press, Boca Raton, FL, 1998.
[6] Riley, J. J. & Maxey, M. R., *Phys. Fluids*, 26, 883, 1983.
[7] Peskin, C.S. & McQueen, D.M., *J. Comput. Phys.*, 81, 372, 1989.
[8] Sundaram, S. & Collins, L. R., *J. Fluid Mech.*, 335, 75, 1997.